

Loss-of-function mutations and inducible RNAi suppression of Arabidopsis *LCB2* genes reveal the critical role of sphingolipids in gametophytic and sporophytic cell viability

Charles R. Dietrich^{1,†}, Gongshe Han², Ming Chen³, R. Howard Berg³, Teresa M. Dunn² and Edgar B. Cahoon^{1,*,‡}

¹USDA-ARS Plant Genetics Research Unit, Donald Danforth Plant Science Center, 975 N. Warson Road, St Louis, MO 63132, USA,

²Department of Biochemistry and Molecular Biology, Uniformed Services University of the Health Sciences, 9701 Jones Bridge Road, Bethesda, MD 20814, USA, and

³Donald Danforth Plant Science Center, 975 N. Warson Road, Saint Louis, MO 63132, USA

Received 2 November 2007; revised 13 December 2007; accepted 19 December 2007.

*For correspondence (fax +1 314 587 1391; e-mail ecahoon@danforthcenter.org).

†Present address: Monsanto Company, 700 Chesterfield Parkway West, St Louis, MO 63198, USA.

‡Present address: Donald Danforth Plant Science Center, 975 N. Warson Road, St Louis, MO 63132, USA.

Summary

Serine palmitoyltransferase (SPT) catalyzes the first step in sphingolipid biosynthesis, and downregulation of this enzyme provides a means for exploring sphingolipid function in cells. We have previously demonstrated that Arabidopsis SPT requires LCB1 and LCB2 subunits for activity, as is the case in other eukaryotes. In this study, we show that Arabidopsis has two genes (*AtLCB2a* and *AtLCB2b*) that encode functional isoforms of the LCB2 subunit. No alterations in sphingolipid content or growth were observed in T-DNA mutants for either gene, but homozygous double mutants were not recoverable, suggesting that these genes are functionally redundant. Reciprocal crosses conducted with *Atlcb2a* and *Atlcb2b* mutants indicated that lethality is associated primarily with the inability to transmit the *lcb2* null genotype through the haploid pollen. Consistent with this, approximately 50% of the pollen obtained from plants homozygous for a mutation in one gene and heterozygous for a mutation in the second gene arrested during transition from uni-nucleate microspore to bicellular pollen. Ultrastructural analyses revealed that these pollen grains contained aberrant endomembranes and lacked an intine layer. To examine sphingolipid function in sporophytic cells, Arabidopsis lines were generated that allowed inducible RNAi silencing of *AtLCB2b* in an *Atlcb2a* mutant background. Studies conducted with these lines demonstrated that sphingolipids are essential throughout plant development, and that lethality resulting from *LCB2* silencing in seedlings could be partially rescued by supplying exogenous long-chain bases. Overall, these studies provide insights into the genetic and biochemical properties of SPT and sphingolipid function in Arabidopsis.

Keywords: sphingolipid, ceramide, long-chain base, pollen, endomembrane.

Introduction

Sphingolipids are major components of endomembranes, including plasma membrane, tonoplast and the Golgi apparatus, and are enriched along with sterols in detergent-resistant membranes or 'lipid rafts' in plasma membranes (Borner *et al.*, 2005; Laloi *et al.*, 2007; Mongrand *et al.*, 2004; Sperling *et al.*, 2005; Verhoek *et al.*, 1983). Lipid rafts have been linked with the trafficking and sorting of proteins such as glycosylphosphatidylinositol-anchored

proteins and multi-drug resistance-like proteins that are involved in cell-surface activities such as cell-wall deposition and auxin transport (Borner *et al.*, 2005). In addition, sphingolipid metabolites, including long-chain base-1-phosphates and ceramides, have been implicated in the regulation of cellular processes such as ABA-dependent guard-cell closure and programmed cell death (Coursol *et al.*, 2003, 2005; Liang *et al.*, 2003; Ng *et al.*, 2001;

Spassieva *et al.*, 2002; Townley *et al.*, 2005; Wang *et al.*, 1996).

Long-chain bases are a unique component of sphingolipids. These molecules typically contain 18 carbon atoms in plants and are formed from the condensation of serine and palmitoyl CoA (Lynch and Dunn, 2004). This reaction is catalyzed by the pyridoxal phosphate-dependent enzyme serine palmitoyltransferase (SPT; EC 2.3.1.50). Long-chain bases in plants contain two or three hydroxyl groups and up to two double bonds, although diunsaturated long-chain bases are typically not abundant in sphingolipids from Arabidopsis. The long-chain base is bound through an amide linkage to a fatty acid that ranges in chain length from 16 to 26 carbon atoms to form the ceramide backbone of complex sphingolipids. In plants, the C1 hydroxyl group of the long-chain base component of the ceramide can be substituted with glucose to form glucosylceramides, or with a phosphoinositol head group containing various sugar residues to form the more abundant glycosylphosphoinositol ceramides (Markham *et al.*, 2006).

SPT occurs as a soluble homodimer in some bacteria, including species of the *Sphingomonas* genus (Ikushiro *et al.*, 2001). In all eukaryotes studied to date, SPT is an ER-associated heteromeric protein that consists of LCB1 and LCB2 subunits (Hanada, 2003). We have recently shown that Arabidopsis SPT has a similar subunit configuration (Chen *et al.*, 2006). The catalytic lysine residue that binds pyridoxal phosphate is located in the LCB2 subunit. LCB1 is believed to stabilize LCB2, and the SPT active site is believed to occur at the interface of the dimerized LCB1 and LCB2 subunits (Gable *et al.*, 2002).

Because SPT catalyzes the first step in sphingolipid biosynthesis, mutants and RNAi suppression lines for the LCB1 and LCB2 subunits have been the focus of studies that have examined sphingolipid function. In most eukaryotes, complete suppression of LCB1 or LCB2 expression results in loss of viability, indicating that sphingolipids are essential molecules (Adachi-Yamada *et al.*, 1999; Buede *et al.*, 1991; Chen *et al.*, 2006; Hanada *et al.*, 1992; Nagiec *et al.*, 1994). Examples of defects associated with reduced sphingolipid synthesis include hereditary sensory neuropathy type I, which results from mutations in the LCB1 subunit (Bejaoui *et al.*, 2002). Interestingly, null mutants of LCB2 in the trypanosome protozoa *Leishmania* are viable but are unable to differentiate into parasitic forms, apparently due to defects in sphingolipid-associated membrane-trafficking (Zhang *et al.*, 2003).

We have recently examined the effects of complete and partial downregulation of Arabidopsis LCB1 (Chen *et al.*, 2006). Homozygous T-DNA mutants for the single *AtLCB1* gene in Arabidopsis were not recoverable, which is consistent with an essential role of sphingolipids in plants, at least during the reproductive stages of plant growth (Chen *et al.*, 2006). In addition, partial suppression of *AtLCB1* by RNAi

resulted in plants with marked reductions in growth, altered leaf morphology, and the development of necrotic lesions on mature leaves. Despite these phenotypes, the total content of sphingolipids in leaves of these plants on a dry weight basis was not reduced (Chen *et al.*, 2006). These results indicated that plants are able to adjust their growth to compensate for reductions in sphingolipid synthesis.

The impact of suppressed expression of the LCB2 subunit of Arabidopsis SPT has yet to be examined. Tamura *et al.* (2001) have previously reported characterization of one of the Arabidopsis *LCB2* genes (*At5g23670*). It was shown that the corresponding polypeptide is ER-localized, as is the Arabidopsis LCB1 subunit (Chen *et al.*, 2006), and expression of this Arabidopsis LCB2 in a yeast *lcb2Δ* mutant increased SPT activity (Tamura *et al.*, 2001). Chen *et al.* (2006) also demonstrated that co-expression of this Arabidopsis LCB2 subunit along with Arabidopsis LCB1 resulted in sufficient SPT activity to complement the long-chain auxotrophy of various yeast SPT mutants. In the studies reported here, we show that Arabidopsis contains two functional genes for the LCB2 subunit of SPT. We also show that these genes are redundant, and null mutants of both genes display gametophytic lethality, characterized by alterations in the endomembrane system of pollen. Furthermore, by development and use of an inducible RNAi system for silencing of LCB2 gene expression, we provide evidence that sphingolipid synthesis is required during multiple stages of plant development, and not just during gametophyte and embryo development. Analyses of these LCB2 loss-of-function mutants provide new insights into the role of sphingolipids in plant growth and development, and complement ongoing studies of sphingolipid function in other eukaryotes, including yeast and mammals.

Results

Arabidopsis contains two functional LCB2 genes

Although sphingolipids are major structural components of membranes, their functional significance is still not well defined in plant cells. To obtain more information about sphingolipid function, Arabidopsis SPT was targeted for downregulation because this enzyme catalyzes the first committed step in sphingolipid synthesis. The studies presented here focus on the LCB2 subunit of SPT because it contains the catalytically essential Lys residue of SPT, and, in mammalian and yeast cells, LCB2 appears to be under greater post-transcriptional regulation than LCB1 (Gable *et al.*, 2000; Han *et al.*, 2004; Yasuda *et al.*, 2003). As a prelude to these studies, the genes for Arabidopsis LCB2 were identified, and studies were conducted to determine their relative contributions to sphingolipid synthesis in Arabidopsis.

Searches of the Arabidopsis genome revealed two genes with significant homology to the yeast LCB2 subunit of SPT: At5g23670, designated *AtLCB2a*, and At3g48780, designated *AtLCB2b*. These genes have absolute conservation of intron/exon junctions and encode 489 amino acid polypeptides that share 89% identity and 47% identity with yeast LCB2. A third LCB2-like sequence is present in Arabidopsis tandem to *AtLCB2b* at chromosome position At3g48790. This gene, however, appears to be a pseudogene, as it is only a partial duplicate of *AtLCB2b* and there is no evidence from EST data that a transcript is produced from it. At3g48790 encodes a 350 amino acid polypeptide that shares 78% and 82% identity with the C-terminal portions of *AtLCB2a* and *AtLCB2b*, respectively.

A cDNA corresponding to At5g23670 (*AtLCB2a*) was previously confirmed to be a functional LCB2 subunit by yeast expression experiments, including complementation of yeast LCB2 mutants (Chen *et al.*, 2006; Tamura *et al.*, 2001). To determine whether the *AtLCB2b* gene also encodes a functional LCB2 subunit, the corresponding cDNA was co-expressed with the cDNA for the Arabidopsis LCB1 subunit in yeast *lcb1Δ/lcb2Δ* mutants, and shown to rescue the long-chain base auxotrophy of these cells (Figure 1a). These results indicate that both *AtLCB2a* and *AtLCB2b* are

functional LCB2 subunits. In addition, the activity of SPT in microsomal extracts from yeast mutants co-expressing *AtLCB1/AtLCB2a* and *AtLCB1/AtLCB2b* was nearly equivalent (Figure 1b), suggesting that *AtLCB2a* and *AtLCB2b* are biochemically capable of functional redundancy in Arabidopsis.

AtLCB2a and AtLCB2b are ubiquitously expressed in Arabidopsis

Expression patterns of the two *AtLCB2* genes were examined as an additional approach to determine whether these genes have distinct or redundant roles in Arabidopsis plants. Northern blot analyses were performed using probes specific for *AtLCB2a* and *AtLCB2b* (Figure 2). Transcripts for both genes were detected in all organs, with the highest expression in flowers. However, expression patterns for the two genes, although similar, were not identical. The *AtLCB2a* transcript was present at higher levels than the *AtLCB2b* transcript in all organs analyzed. In addition, the level of *AtLCB2a* transcript, in contrast to that of *AtLCB2b*, was elevated in roots. The *AtLCB2b* transcript also was found at its highest level in mature flowers but to a lower level in flower buds, while *AtLCB2a* transcript levels

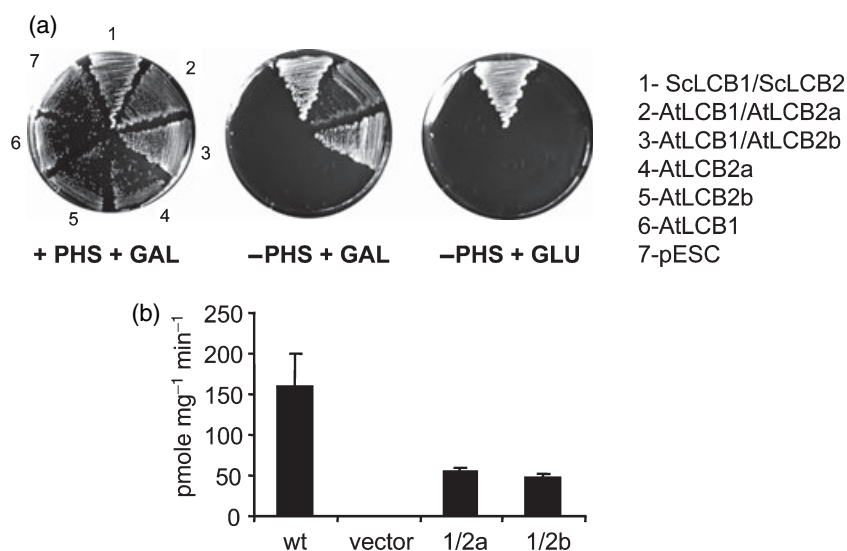


Figure 1. Co-expression of *AtLCB2a* and *AtLCB2b* with *AtLCB1* complements the long-chain base auxotrophy of a *Saccharomyces cerevisiae* SPT *lcb1Δ/lcb2Δ* mutant.

(a) Complementation studies were performed using a *S. cerevisiae lcb1Δ/lcb2Δ* strain that is a sphingolipid long-chain base auxotroph. cDNAs for *AtLCB2a* and *AtLCB2b* were placed under the control of the *GAL10* promoter alone or together with the *AtLCB1* cDNA under the control of the *GAL1* promoter in the yeast expression vector pESC-URA. The *Δlcb1Δ/lcb2Δ* strain was transformed with galactose-inducible expression plasmids containing cDNAs for *AtLCB1/AtLCB2a*, *AtLCB1/AtLCB2b*, *AtLCB1*, *AtLCB2a*, *AtLCB2b* and the pESC vector. The *lcb1Δ/lcb2Δ* strain was also co-transformed with plasmids containing the yeast ScLCB1 and ScLCB2 genes expressed from their native promoters. The transformed cells were grown on media supplemented as shown: (i) with the long-chain base phytosphingosine and galactose (+PHS +GAL), (ii) with galactose but no phytosphingosine (-PHS +GAL), and (iii) with glucose but no phytosphingosine (-PHS +GLU). Growth of cells co-expressing *AtLCB1/AtLCB2a* and *AtLCB1/AtLCB2b* on -PHS+GAL medium indicates complementation of the long-chain base auxotrophy of the *lcb1Δ/lcb2Δ* strain.

(b) SPT activity was measured in microsomes isolated from the *lcb1Δ/lcb2Δ* mutant harboring the ScLCB1 and ScLCB2 plasmids (WT), the pESC vector (vector), and the *AtLCB1/AtLCB2a* (1/2a) and *AtLCB1/AtLCB2b* (1/2b) co-expression constructs ($n = 3$, means and SD). Cells were grown in galactose-induction medium without long-chain base supplementation (wild-type, 1/2a and 1/2b) or supplemented with phytosphingosine (vector).

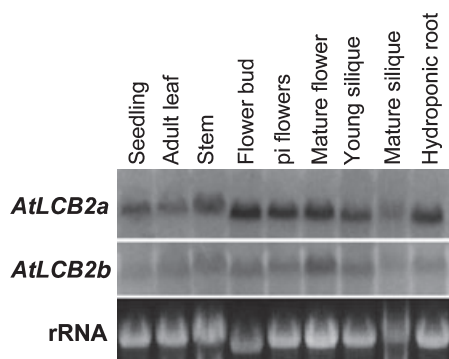


Figure 2. Expression of *AtLCB2a* and *AtLCB2b* in various organs of Arabidopsis.

Northern blot analyses for *AtLCB2a* and *AtLCB2b* expression in Arabidopsis organs at various growth stages. Hybridization was first performed using an *AtLCB2a*-specific probe, and the blot was re-hybridized with an *AtLCB2b*-specific probe. RNA samples were taken from 10-day-old soil-grown seedlings and from mature plants. Mature flowers contained visible pistils. Siliques at 3–7 days post-anthesis were collected for the young silique sample, and fully elongated siliques prior to senescence were collected for the mature silique sample. All samples were from wild-type Col-0, except for the *pi* flower sample, which is from the inflorescence of a *pistillata indeterminate (pi)* mutant. Ethidium bromide-stained 40S ribosomal bands are shown below to confirm equal loading.

were high in both mature flowers and flower buds (Figure 2). Furthermore, analysis of RNA isolated from the *pistillata (pi)* mutant, which lacks stamens (Bowman *et al.*, 1989), indicated that levels of the *AtLCB2b* transcript are lower in *pi* flowers than in flowers from wild-type plants. This suggests that the stamen is a major contributor to the *AtLCB2b* expression detected in flowers from wild-type plants. In contrast, *AtLCB2a* expression appears to be distributed among the multiple flower parts, as expression of this gene is similar in flowers from *pi* and wild-type plants. Consistent with these results, microarray data from the GENEVESTIGATOR database (Zimmermann *et al.*, 2004) also show that the relative expression of *AtLCB2a* and *AtLCB2b* in stamens as well as pollen is higher than in other organs of Arabidopsis (Figure S1).

Analysis of Arabidopsis plants carrying GUS fusion constructs with promoter sequences for each of the *LCB2* genes also revealed these differences in floral expression. For example, *AtLCB2b* promoter-mediated GUS expression in young flower buds was initially restricted to developing pollen spores within the stamen and is not detected in the petals, glumes or petiole until the flowers are mature (Figure 3a,b). In contrast, expression mediated by the *AtLCB2a* promoter was detected at high levels in the petiole, sepals and petals in young flowers, but was not detected in the anthers during the early stages of pollen development (Figure 3c,d). GUS analysis also revealed subtle differences in expression of the two genes within the pistil. *AtLCB2b* promoter-driven GUS expression, for example, was not detected in the pistil of unfertilized flowers but appears after

fertilization, specifically in the funiculi (Figure 3e–g). Conversely, *AtLCB2a* promoter-mediated GUS expression was detected strongly in the stigma region of the pistil in young flowers but staining was not seen in the funiculi (Figure 3h, and data not shown). In seedlings, *AtLCB2a* promoter:GUS expression was detected throughout the leaves and roots (Figure 3i,j), while *AtLCB2b* promoter:GUS expression was detected only weakly in leaves but strongly in the root tip (Figure 3k,l).

Overall, these results indicate that both *LCB2* genes are expressed ubiquitously in Arabidopsis, although *AtLCB2a* expression is higher than that of *AtLCB2b* in most portions of the plant. In addition, differences in expression levels of *AtLCB2a* and *AtLCB2b* are detectable within specific organs (e.g. flowers), but distinct spatial separation of the expression of these genes between organs is not evident.

Characterization of T-DNA insertion alleles

Arabidopsis lines that have T-DNA insertions in either the *AtLCB2a* or *AtLCB2b* gene were obtained, and the insertion sites were confirmed by sequence analysis of the PCR product amplified using the T-DNA left border (LB) and a gene-specific primer. Three T-DNA insertion lines were characterized for *AtLCB2a* (SALK_061472, *Atlcb2a-1*; SAIL 706-A05, *Atlcb2a-2*; GABI 216-D07, *Atlcb2a-3*), and one line was characterized for *AtLCB2b* (SALK_110242, *Atlcb2b-1*; Figure 4a). RNA isolated from homozygous plants was tested by RT-PCR to confirm that each insertion resulted in the absence of detectable transcript accumulation of the respective gene (Figure 4b). Plants homozygous for either the *AtLCB2a* T-DNA insertion alleles or the *AtLCB2b* T-DNA allele showed no apparent differences in growth or development in comparison to wild-type plants (data not shown).

To determine whether either single mutation affects sphingolipid composition, the total long-chain base extracts for wild-type, *Atlcb2a-1*, and *Atlcb2b-1* plants were analyzed. Leaves from wild-type Arabidopsis contain six distinct long-chain base species (Table 1). The *cis* (*E*) and *trans* (*Z*) isomers of t18:1 account for approximately 85% of the total long-chain bases, with t18:0, d18:1Z, d18:1E and d18:0 accounting for the remaining long-chain bases. All of the *AtLCB2* mutants had very similar long-chain base compositions, with the only significant difference being a slight increase in the percentage of t18:0 in both mutants (Table 1). The total long-chain base content for wild-type Arabidopsis leaves was 2.05 ± 0.28 nmol/mg DW ($n = 3$, mean \pm SD). The total long-chain base contents for the *Atlcb2a-1* and *Atlcb2b-1* mutants were 1.71 ± 0.13 ($n = 3$) and 1.87 ± 0.26 nmol/mg DW ($n = 3$), respectively. These values are not significantly different from the long-chain base content in leaves from wild-type plants, and indicate that T-DNA disruption of one *AtLCB2* gene does not result in significant reductions in long-chain base content. The

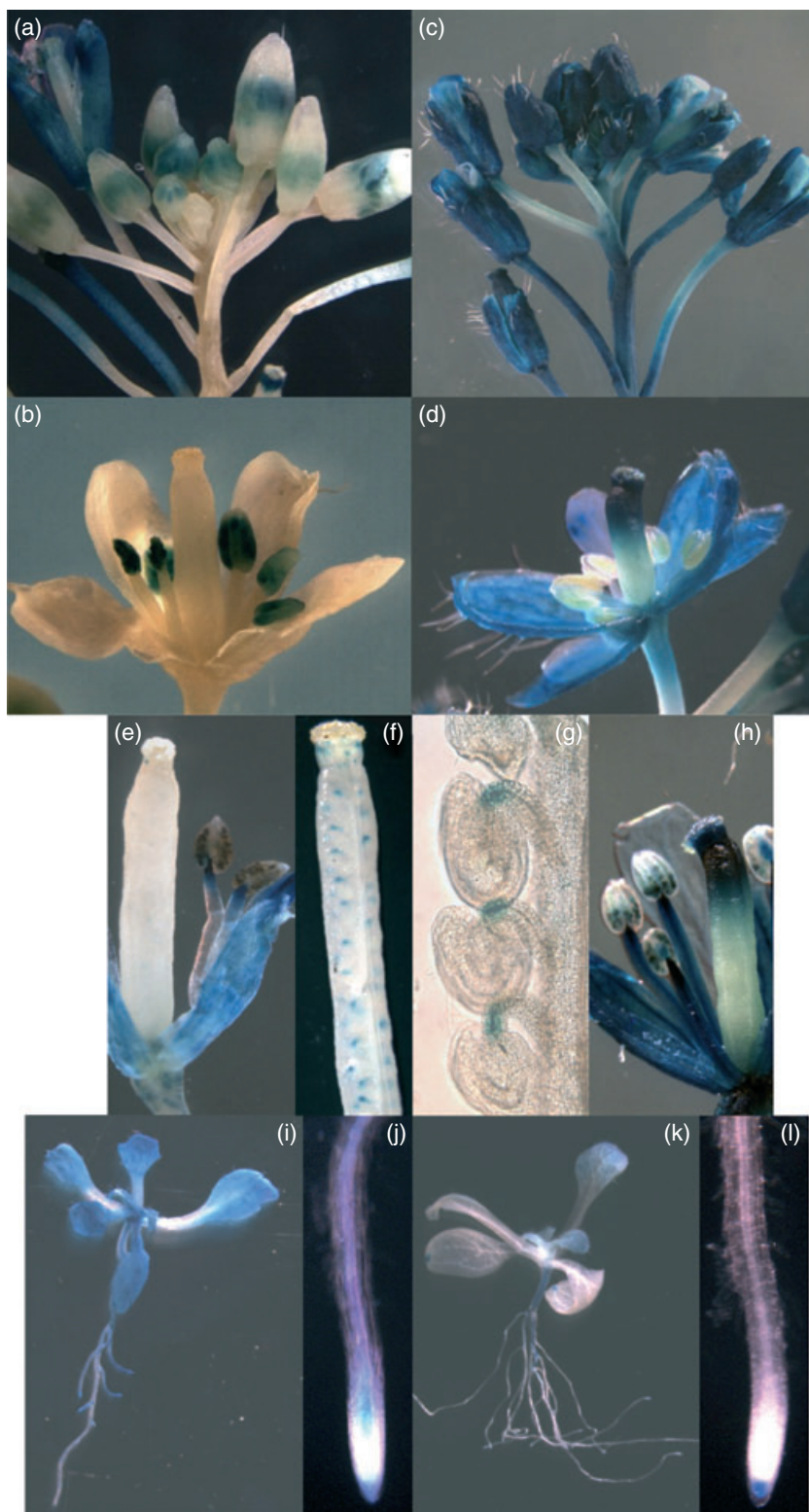


Figure 3. GUS expression analysis for *AtLCB2a* and *AtLCB2b* promoters. Comparison of *AtLCB2a* and *AtLCB2b* expression patterns for promoter:GUS fusion constructs. *AtLCB2b* promoter-mediated expression of GUS in (a) an inflorescence, (b) an immature flower that has been opened, (e) a mature flower, and (f) a pistil from a mature flower; funiculus staining in (g) developing seeds, (k) seedling and (l) root tip. *AtLCB2a* promoter-mediated expression of GUS in (c) an inflorescence, (d) an immature flower that has been opened, (h) a mature flower, (i) a seedling, and (j) a seedling root tip.

similar long-chain base compositions and contents between mutants and wild-type plants indicate that the two *AtLCB2* genes are redundant and loss of one gene is compensated for by expression of the second gene. Based on quantitative

RT-PCR performed on RNA from seedlings, this compensation does not appear to be due to changes in transcription, because *AtLCB2a* expression is not significantly increased in *AtLCB2b* mutants and vice versa (data not shown).

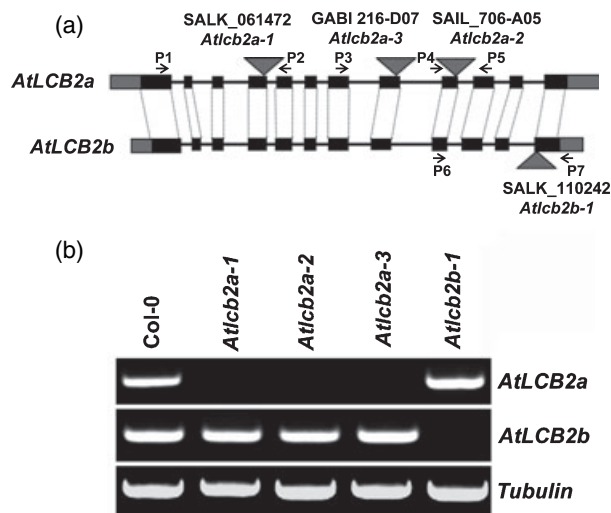


Figure 4. T-DNA insertion mutants of *AtLCB2a* and *AtLCB2b*. (a) Structures of the T-DNA mutants for *AtLCB2a* and *AtLCB2b* used in these studies. The positions of T-DNA insertions are indicated by inverted triangles. Exons are indicated by solid boxes, introns are shown as black lines, and 5' and 3' untranslated regions are shown in grey. The positions of primers used for determining the expression of *AtLCB2a* and *AtLCB2b* in T-DNA mutants are indicated by arrows with the accompanying primer name. The primers shown were confirmed to yield products of the expected size in RT-PCR experiments with wild-type plants (data not shown). (b) RT-PCR analysis of *AtLCB2a* and *AtLCB2b* expression in leaves of wild-type plants (Col-0) and T-DNA mutants for each gene. Expression of *AtLCB2a* was assessed using primers P1 and P2 [as shown in (a)] for wild-type, *AtLCB2a-1* and *AtLCB2b-1*, primers P3 and P5 for *AtLCB2a-3*, and primers P4 and P5 for *AtLCB2a-2*. Expression of *AtLCB2b* was assessed using primers P6 and P7. The quality of cDNA from wild-type and T-DNA mutant plants was confirmed by RT-PCR experiments using primers specific for the β -tubulin gene *TUB1* (*Tubulin*).

AtLCB2a and *AtLCB2b* are redundant genes

To test for gene redundancy, crosses were made between plants containing the *AtLCB2a-1* and *AtLCB2b-1* mutant alleles. From these crosses, double heterozygous plants were identified and taken to the F_2 generation in order to obtain double mutant progeny at an expected frequency of 1/16. PCR genotyping of 88 F_2 progeny, however, did not identify any plants with the double mutant genotype (Table 2). To increase the expected frequency of recovering plants with the double mutant genotype, F_3 progeny from plants that were homozygous for one mutation and hetero-

zygous for the other were analyzed. One quarter of the progeny from these plants would be expected to be a double mutant, yet genotyping of 215 individual F_3 progeny from a plant homozygous for the *AtLCB2a-1* mutant and heterozygous for *AtLCB2b-1* mutant (i.e. aaBb) and 202 F_3 progeny from a plant homozygous for the *AtLCB2b-1* mutant and heterozygous for the *AtLCB2a-1* mutant (i.e. Aabb) failed to identify a single double mutant plant (Table 2). In addition, the observed genotypic ratios were statistically different from the expected ratios when calculated using a full genotypic ratio or a ratio adjusted to account for embryo lethality (Table 2, and data not shown). These results suggest gametophytic lethality.

LCB2 is required for normal gametophyte development

Reciprocal crosses were performed using plants of the aaBb or Aabb genotype to test for gametophytic lethality (Table 3). One-half of the progeny from these crosses would be expected to carry both mutant alleles, i.e. have the AaBb genotype. However, when these plants were used as the pollen (male) source to cross with wild-type plants, none of the resulting progeny carried both mutant alleles. This indicates that pollen with the double hemizygous mutant genotype (ab) is either non-viable or does not participate in fertilization. When these same plants were used as females to cross with pollen from wild-type plants, progeny were recovered that carried both mutant alleles, although at less than the expected frequency of 50%. Transmission through the female gametophyte was 20% when the female genotype was aaBb and 25% when the female genotype was Aabb. The results from these reciprocal crosses reveal that the failure to recover double *AtLCB2a/AtLCB2b* mutants is not due to embryo lethality but instead is due to inability to transmit the double mutant genotype through the haploid pollen.

To confirm these results, the *AtLCB2b-1* mutant was crossed with a second mutant allele of *AtLCB2a* (*AtLCB2a-2*, SAIL_706-A05), and similar analyses were performed. Consistent with the data detailed above, double mutant plants were not recovered, due again to failure of the double haploid mutant genotype to transmit through the male gametophyte (Tables S1 and S2). Transmission through the female gametophyte was again reduced, but, with this allele

Table 1 Sphingolipid long-chain base composition (mol%) of leaves from wild-type (Col-0) and *AtLCB2a-1* and *AtLCB2b-1* plants

	t18:1(Z)	t18:1(E)	t18:0	d18:1(Z)	d18:1(E)	d18:0
Wild-type	22.2 \pm 0.8	62.9 \pm 1.0	5.4 \pm 0.2	1.1 \pm 0.2	7.4 \pm 0.9	0.7 \pm 0.2
<i>AtLCB2a</i>	21.5 \pm 1.0	61.7 \pm 1.2	7.3 \pm 0.1	1.0 \pm 0.1	7.3 \pm 0.8	0.9 \pm 0.1
<i>AtLCB2b</i>	21.7 \pm 0.7	62.1 \pm 0.6	6.4 \pm 0.3	1.0 \pm 0.1	7.5 \pm 0.6	0.9 \pm 0.1

Each value is the mean of three or four independent measurements \pm SD.

Abbreviations: t18:1(E or Z), 4-hydroxy-8-(trans or cis)-sphinganine; t18:0, 4-hydroxysphinganine or phytosphingosine; d18:1(E or Z), 8-(trans or cis)-sphinganine; d18:0, sphinganine or dihydrosphingosine.

Table 2 Segregation analysis of F₂ and F₃ progeny from plants carrying *AtLCB2* mutant alleles

Parent genotype ^a	Progeny genotype (observed/expected) ^b									Total
	AABB	AaBB	AABb	AaBb	aaBB	aaBb	AAbb	Aabb	aabb	
F ₂ – AaBb ^{c,e}	5/5.5	14/11	18/11	27/22	8/5.5	4/11	7/5.5	5/11	0/5.5	88
F ₃ – aaBb ^{d,e}	N/A ^f	N/A	N/A	N/A	165/54	50/108	N/A	N/A	0/54	215
F ₃ – Aabb ^{d,e}	N/A	N/A	N/A	N/A	N/A	N/A	154/51	48/101	0/51	202

^aAn upper-case letter indicates the wild-type allele of *AtLCB2a* (A) and *AtLCB2b* (B). A lower-case letter indicates the mutant alleles for *Atlcb2a-1* (a) and *Atlcb2b-1* (b).

^bProgeny genotypes were determined by PCR analysis.

^cGenotyping results of 88 individual F₂ progeny from doubly heterozygous parent plants.

^dGenotyping results of F₃ progeny from parent lines homozygous for one mutant allele and heterozygous for the other.

^e χ^2 analysis indicates that the observed genotypic ratios are statistically different at the 99% confidence interval from the expected genotypic ratio for this population.

^fN/A, the designated genotype is not obtainable from the parent plants used.

Table 3 Segregation analysis of progeny from reciprocal crosses of plants carrying mutant *AtLCB2* alleles

Parent genotype ^a	Progeny genotype (observed/expected) ^b			Total
	AaBb	AaBB	AABb	
aaBb – female ^{c,e}	49/123	197/123	N/A ^f	246
aaBb – male ^{d,e}	0/67	134/67	N/A	134
Aabb – female ^{c,e}	59/118	N/A	177/118	236
Aabb – male ^{d,e}	0/43	N/A	86/43	86

^aAn upper-case letter indicates the wild-type allele of *AtLCB2a* (A) and *AtLCB2b* (B). A lower-case letter indicates the mutant alleles for *Atlcb2a-1* (a) and *Atlcb2b-1* (b).

^bProgeny genotypes were determined by PCR analysis.

^cFlowers from plants with the indicated genotypes were emasculated and pollinated using pollen from a wild-type plant.

^dPlants with indicated genotypes were used to pollinate emasculated flowers from wild-type plants.

^e χ^2 analysis indicates that the observed genotypic ratios are statistically different at the 99% confidence interval from the expected genotypic ratio for this population.

^fN/A, the designated genotype is not obtainable from the parent plants used.

combination, transmission through the female was 43% when either aaBb or Aabb were pollinated with wild-type pollen (Table S2). These results indicate that penetrance of the double *LCB2*-null alleles through the female gametophyte is variable, based on the differing rates of transmission through the female between the allele combinations shown in Table 2 and Table S2. This variability was evident in siliques from self-pollinated plants. Siliques contained normal seeds in addition to apparently unfertilized ovules and embryos arrested at the zygotic stage (Figure S2).

LCB2 is required for pollen development

To determine the basis for the lack of pollen transmission of both mutant alleles, viability staining was performed with pollen from plants with aaBb and Aabb genotypes.

Approximately 50% of the pollen from these mutants was non-viable. This phenotype was observed for combinations of *Atlcb2a-1/Atlcb2b-1* and *Atlcb2a-2/Atlcb2b-1* mutant alleles. In contrast, >99% of the pollen was viable from wild-type plants and plants homozygous for T-DNA insertions in either *AtLCB2* gene (Figure 5a,b, and data not shown).

To further characterize this phenotype, 4',6-diamidino-2-phenylindole (DAPI)-stained pollen from wild-type and mutant plants at various stages of development was observed using white-light and epifluorescence microscopy. Pollen from plants with T-DNA insertions in either gene appeared the same as that from wild-type plants at the unicellular, bicellular and tricellular stages of development (data not shown). In mutant plants with the aaBb or Aabb genotype, nearly all of the unicellular microspores were similar to those of wild-type plants at the earliest stages of development. At this point in development, microspores from the aaBb, Aabb and wild-type plants contained a single generative nucleus (Figure 5c–f). However, marked differences were observed between pollen from wild-type and double mutant plants at the subsequent bicellular stage of development (Figure 5g–j). At this stage, most pollen from wild-type plants contained a large vegetative nucleus and a single generative nucleus (Figure 5h). In contrast, approximately 50% of the pollen at this stage in the homozygous/heterozygous double mutant allele plants (i.e. aaBb and Aabb) lacked DAPI-stained nuclei (Figure 5j), and the pollen was about half the size of that from wild-type plants (Figure 5g versus Figure 5i). These differences were also observed in pollen at the later tricellular stage (Figure 5k–n). At this point in development, pollen from wild-type plants had two intensely stained generative nuclei and one diffusely stained vegetative nucleus (Figure 5l). Similar to the bicellular stage, approximately 50% of the pollen from the homozygous/heterozygous double mutant allele plants was smaller and did not have the typical tri-nucleate DAPI staining pattern (Figure 5n). Most of these small pollen grains did not stain with DAPI, although occasional diffuse

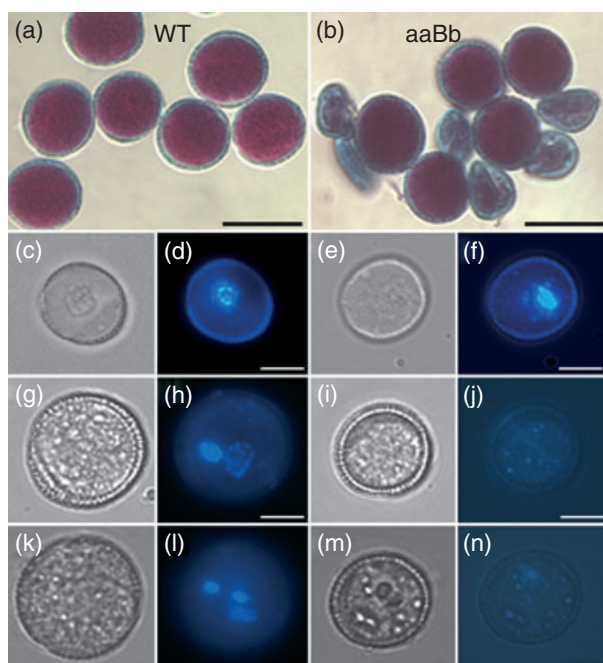


Figure 5. Pollen development in wild-type and mutant plants.

Pollen viability was assessed using Alexander's stain for (a) wild-type plants and (b) plants genotyped as homozygous for the *AtLCB2a-1* mutant allele and heterozygous for the *AtLCB2b-1* mutant allele (i.e. aaBb). Red pollen grains are viable; shrunken green pollen grains are non-viable. (c–n) DAPI-stained pollen grains were observed using white-light (c, g, k, e, i, m) and epifluorescence (d, h, l, f, j, n) microscopy. Pollen from wild-type plants at (c, d) the unicellular microspore stage, (g, h) the bicellular pollen stage, and (k, l) the tricellular pollen stage, and pollen from mutant plants at (e, f) the unicellular microspore stage, (i, j) the bicellular pollen stage, and (m, n) the tricellular pollen stage. Similar patterns of viability and DAPI staining were observed for pollen from plants heterozygous for the *AtLCB2a-1* mutant allele and homozygous for the *AtLCB2b-1* mutant allele (i.e. Aabb) as well as for the corresponding combinations of *AtLCB2a-2* and *AtLCB2b-1* mutant alleles. Scale bars = 20 μ m (a, b) and 10 μ m (c–n).

staining was observed. These results indicate that loss of pollen viability arises early in pollen development during transition from the uni-nucleate microspore to the bicellular pollen grain, suggesting that sphingolipids are particularly important at this stage in development.

Transmission electron microscopy of developing pollen identified indicators of gametophytic lethality between the unicellular microspores and the bicellular pollen stage. Anthers from plants genotyped as homozygous/heterozygous for the mutant alleles (Aabb; i.e. producing 50% mutant pollen) were compared with anthers from the single mutant (AAbb; i.e. producing only normal pollen) and wild-type plants. Developing pollen from the single mutants and wild-type plants was comparable to developing pollen from wild-type *Arabidopsis* as previously described (Owen and Makaroff, 1995). Sections from these plants were used as a reference to identify abnormally developed pollen from Aabb plants at a similar developmental stage. Anthers from Aabb plants with pollen at the bicellular I stage had both

normal pollen and apparently mutant pollen (Figure 6a–c). The normal pollen at this developmental stage had passed through mitosis I. By this stage, the large central vacuole had fragmented and the generative cell was attached to the wall of the vegetative cell (Figure 6b). Mutant microspores were also present that appeared to be arrested at a mid- to late-microspore stage and were presumed to be the double mutant microspores (Figure 6c). The central vacuole in the mutant microspores did not appear to be resorbed, as is the case in normal pollen development. Instead, the vacuole persisted in the microspore and often appeared to contain some internal degradation products. The cytoplasm of these microspores was less dense compared to normal bicellular I pollen, and plastids were dilated and lacked oil droplets found in normal bicellular I pollen (Figure 6b). Furthermore, the nuclear envelope structure was modified by the formation, in some regions, of vesicles between the inner and outer membrane (Figure 6f). The absence of heterochromatin correlates with the lack of DAPI staining (Figure 5f). These microspores also lacked the intine layer that is present in normal bicellular I pollen (compare Figure 6d and Figure 6e). Deposition of the intine layer is associated with endomembrane components including Golgi stacks and the ER (Figure 6d; Hess, 1993; Nakamura, 1979). The lack of clearly defined ER and Golgi in the mutant pollen (Figure 6e) correlates with the absence of a functioning endomembrane system for deposition of the intine layer. The cytoplasm in the double mutant microspores generally showed lower contrast compared to wild-type cells. In anthers containing wild-type pollen at the tricellular stage, the double mutant pollen was aborted, exhibiting cell death (data not shown). Overall, these observations indicate that the pollen lethality in the double *AtLCB2a/AtLCB2b* mutant is associated with defects in the endomembrane system.

Inducible downregulation of SPT reveals the essential nature of sphingolipids during sporophytic growth

The gametophytic lethality associated with T-DNA disruption of both *AtLCB2* genes precludes the examination of phenotypes arising from loss of sphingolipid production in diploid sporophytic cells. As an alternative approach to examine the sphingolipid requirements of sporophytic cells, an RNAi expression cassette was generated for inducible silencing of *AtLCB2b* in an *AtLCB2a* mutant background. The system used was based on those described by Padidam *et al.* (2003) and Koo *et al.* (2004), and allows induction of an *AtLCB2b*-specific hairpin by application of the ecdysone receptor agonist methoxyfenozide. The genetic elements of this system, which are shown in Figure S3, were assembled into a binary vector conferring hygromycin resistance. To test the efficacy and specificity of this system, the binary vector was transformed into wild-type *Arabidopsis*, and *AtLCB2a* and *AtLCB2b* expression was monitored by RT-PCR

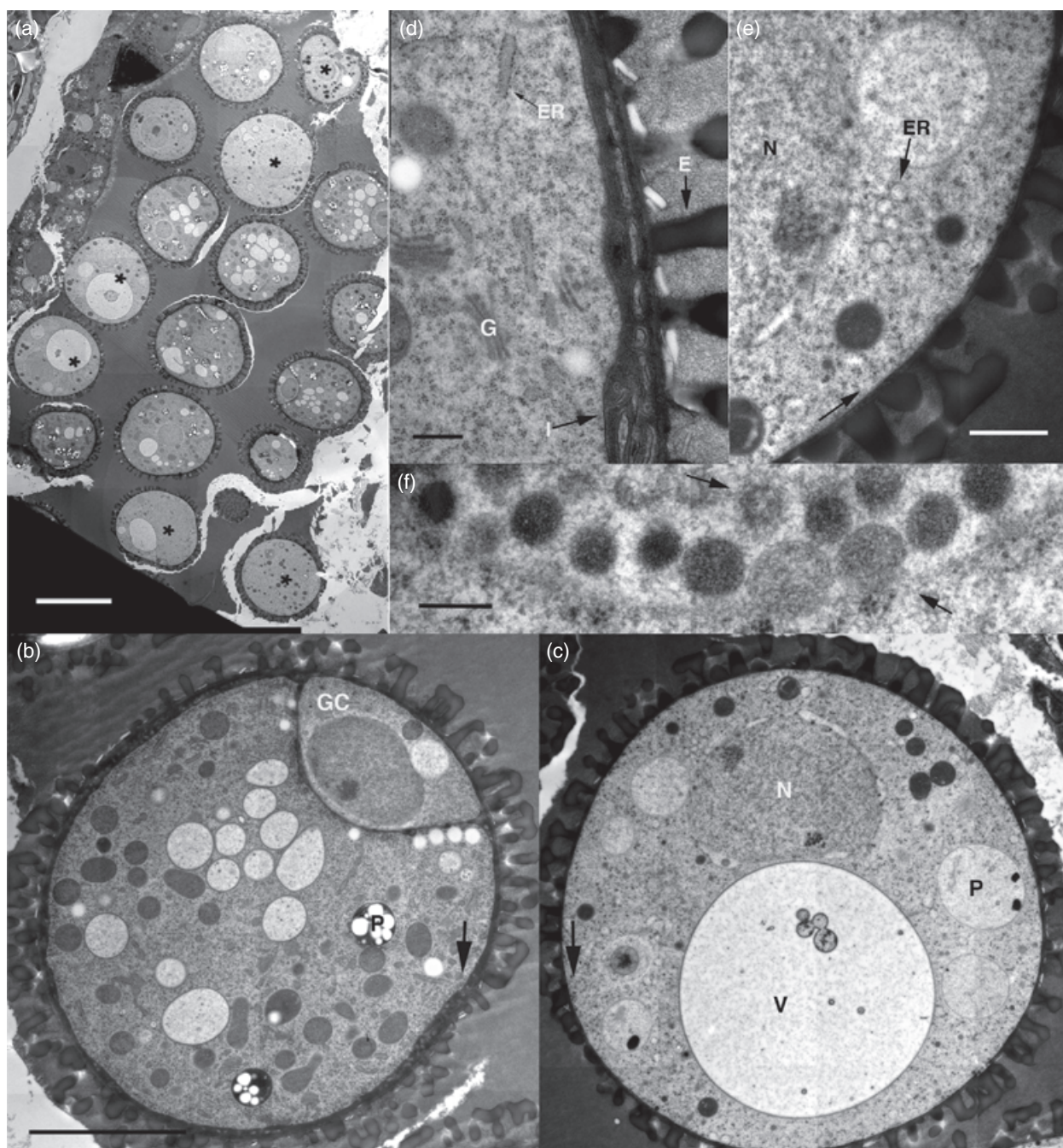


Figure 6. LCB2 is required for intine formation.

Transmission electron microscopy of pollen from plants heterozygous for the *Atlcb2a-2* mutant allele T-DNA insertion and homozygous for the *Atlcb2b-1* mutant allele, which contain 50% aborted pollen.

(a) A single locule containing a mixture of normal and mutant *Atlcb2a-1/Atlcb2b-1* pollen (asterisks); scale bar = 10 μ m.

(b, c) Magnifications from the locule in (a): normal pollen (b) is bicellular (GC, generative cell) with intine (arrow) and plastids (P) containing oil droplets; mutant *Atlcb2a-1/Atlcb2b-1* pollen (c) lacks intine (arrow), and has a prominent vacuole (V) and dilated plastids (P) lacking oil droplets; N, nucleus; scale bars = 5 μ m.

(d, e) Cell wall in normal (d) and mutant (e) pollen. Normal pollen has intine (I) and associated endomembrane components (G, Golgi stacks; ER); mutant pollen lacks intine (arrow) and the ER is vesiculated and ill-defined. Scale bars = 200 nm (d) and 1 μ m (e). (f) The nuclear envelope (bracketed by arrows) in the mutant contains vesicles. Bar = 200 nm.

following application of methoxyfenozide. Gene expression studies conducted three days after application of the inducer showed that *AtLCB2b* expression was downregulated in two

of the three lines examined, but *AtLCB2a* expression was unaffected (Figure S3). These results indicate that the RNAi construct is specific for inducible silencing of *AtLCB2b*.

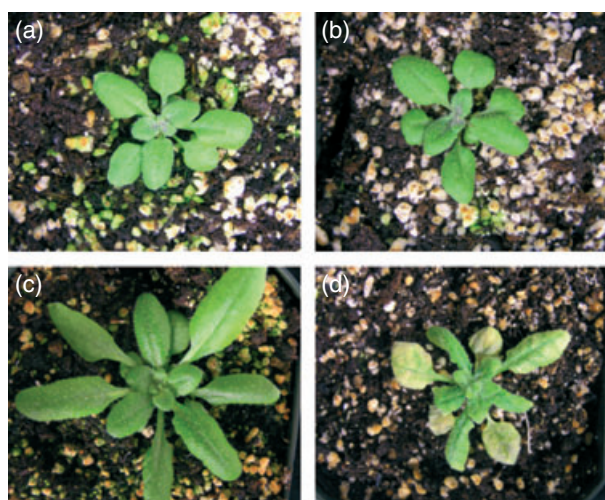


Figure 7. Induced silencing of the *AtLCB2b* gene in an *Atlcb2a-1* mutant background results in lethality.

(a) A 3-week-old non-transformed *Atlcb2a-1* plant and (b) an *Atlcb2a-1* plant transformed with the inducible *AtLCB2b* RNAi construct, before methoxyfenozide induction. (c, d) The same non-transformed (c) and transformed (d) plant at 5 days after induction.

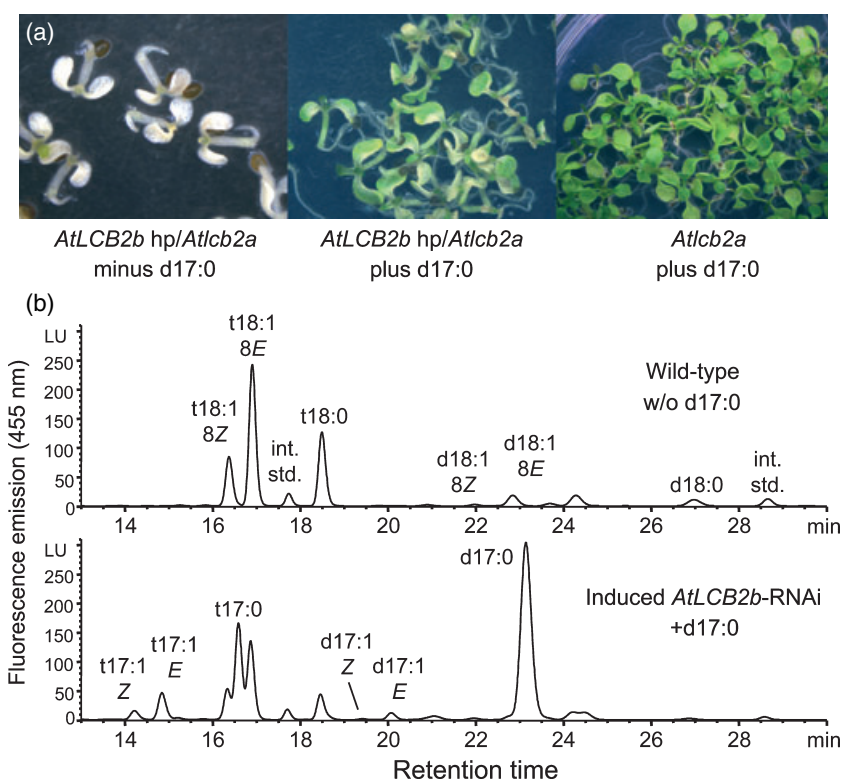
This same binary vector was introduced into a line homozygous for the *Atlcb2a-1* mutant allele. Sixty independent hygromycin-resistant T_1 plants were grown to produce

segregating T_2 lines. Hygromycin-resistant plants from these lines were treated with the methoxyfenozide inducer at 3 weeks old. At 5–7 days post-induction, extensive chlorosis was observed on the expanded portions of leaves (Figure 7), followed by the development of necrotic lesions and eventual death of the plant. A similar phenotype was observed in more than 40 independent lines. In addition, application of the inducer to 10-week-old plants at the latter stages of bolting resulted in a similar pattern of chlorotic patches on leaves followed by necrosis in *Atlcb2a* mutant plants harboring the *AtLCB2b* RNAi transgene (Figure S4). These phenotypes were not observed in response to methoxyfenozide application in wild-type plants or *Atlcb2a-1* mutant plants lacking the inducible *AtLCB2b* RNAi construct. To determine the effect of inducible suppression of *AtLCB2b* on sphingolipid synthesis, the total long-chain base content of leaves from hydroponically grown *Atlcb2a-1* plants was determined at 7 days post-induction. The use of a hydroponic system allowed more uniform delivery of the inducer and more reproducible measurements of long-chain base content. In these studies, the long-chain base content of leaves from *Atlcb2a-1* mutant plants lacking the inducible RNAi construct was 1.37 ± 0.11 nmol mg^{-1} DW ($n = 3$, mean \pm SD) at 7 days post-induction, whereas the long-chain base content of leaves from *Atlcb2a-1* mutant plants with the inducible RNAi construct was 0.88 ± 0.19 nmol mg^{-1} DW ($n = 4$). This indicates that inducible

Figure 8. Complementation of induced *AtLCB2* lethality by growth on medium containing the long-chain base C17 sphinganine.

(a) Seven-day-old seedlings homozygous for the inducible *AtLCB2b*-specific RNAi construct in an *Atlcb2a-1* mutant background, germinated on methoxyfenozide induction medium without exogenous C17 sphinganine (d17:0) long-chain bases (*AtLCB2b* hp/*Atlcb2a* minus d17:0) or with 200 μM d17:0 (*AtLCB2b* hp/*Atlcb2a* plus d17:0). Also shown are seedlings from the *Atlcb2a-1* mutant (lacking the inducible RNAi construct) germinated on induction medium supplemented with long-chain bases (*Atlcb2a* plus d17:0).

(b) HPLC analysis of the long-chain base compositions of sphingolipids from 10-day-old wild-type seedlings grown on medium lacking exogenous d17:0 (wild-type w/o d17:0) and from *Atlcb2a* seedlings containing the inducible *AtLCB2b* RNAi construct on medium with methoxyfenozide and exogenous d17:0 (induced *AtLCB2b*-RNAi +d17:0). Long-chain bases were analyzed as fluorescent derivatives following hydrolysis of sphingolipids.



downregulation of SPT results in significant reductions in long-chain base content.

To confirm that the cell-death phenotype is due to loss of SPT activity, homozygous T_3 lines were grown on medium containing the long-chain base C17 sphinganine (d17:0). *Atlcb2a-1* seeds containing the inducible *AtLCB2b* RNAi construct germinated on medium containing methoxyfenozone without d17:0, but the seedlings had severely reduced root growth and arrested before the emergence of the first true leaves (Figure 8a). At this stage, the seedlings became chlorotic, except in the meristem region which remained green due to lack of RNAi silencing in meristematic cells (Voinnet *et al.*, 1998). By contrast, seedlings grown on induction medium supplemented with d17:0 had normal root growth and partially restored shoot growth (Figure 8a). *Atlcb2a-1* mutant or wild-type plants grown on induction plates appeared normal with or without d17:0 supplementation (Figure 8a, and data not shown). Long-chain base analysis of sphingolipids was conducted on the chemically complemented plants to determine whether the d17:0 was incorporated. These analyses revealed not only d17:0, but also t17:0 and *Z* and *E* isomers of t17:1 and d17:1 (Figure 8b), indicating that the exogenous long-chain bases are indeed incorporated and further metabolized by the seedlings. Overall, these results provide direct evidence that blockage of sphingolipid long-chain base production is the basis for the loss of cell viability. These results also show that sphingolipid synthesis is essential during at least three different sporophytic growth stages: (i) seedling establishment, (ii) in the young plant prior to bolting, and (iii) in the mature plant at later stages of bolting.

Discussion

The LCB2 subunit of serine palmitoyltransferase is encoded by two redundant genes in Arabidopsis

The results from this study and from our previous report (Chen *et al.*, 2006) show that the Arabidopsis LCB2-related polypeptides encoded by At5g23680 (*AtLCB2a*) and At3g48780 (*AtLCB2b*) are able to rescue the long-chain base auxotrophy of yeast serine palmitoyltransferase mutants when co-expressed with the Arabidopsis LCB1 subunit. These findings provide conclusive evidence that the two Arabidopsis genes encode bona fide LCB2 subunits that function as heteromeric proteins with LCB1 to yield an active SPT. In addition, nearly the same SPT activity was detected in microsomes from the complemented yeast expressing either of the Arabidopsis LCB2 polypeptides together with Arabidopsis LCB1. This suggests that the two Arabidopsis LCB2 polypeptides are catalytically redundant in the heteromeric SPT complex. Furthermore, the observations that mutants for either *AtLCB2a* or *AtLCB2b* do not display changes in sphingolipid content or growth phenotypes, yet

double mutants for these genes are not recoverable, indicate that *AtLCB2a* and *AtLCB2b* are functionally redundant.

LCB2 loss-of-function mutant reveals that sphingolipids are essential for gametophytic development

No obvious defects in growth and development were observed in single mutants for either *AtLCB2a* or *AtLCB2b*. Double mutants, however, could not be recovered due to defects in gametophyte development. Reciprocal crossing demonstrated that gametes containing a T-DNA insertion in both genes were 100% non-transmitted through the male gametophyte, and were transmitted at a reduced frequency through the female gametophyte. Gametophytic mutations that affect both male and female gametophyte development typically have a greater impact on pollen rather than ovules (Grini *et al.*, 1999; Johnson *et al.*, 2004). This is probably due to more substantial contributions of the surrounding maternal tissue to female gametophyte development, and may explain the stronger effect of *LCB2*-null mutations on pollen viability.

The gametophytic mutations associated with knockout of both *AtLCB2* genes result in loss of pollen viability early in microspore development, between the unicellular and bicellular microspore stages. This suggests that sphingolipids have an essential role during this period of pollen maturation. One dramatic event that occurs at this stage in wild-type microspores is formation and subsequent resorption of a large central vacuole (Owen and Makaroff, 1995; Yamamoto *et al.*, 2003). As shown in Figure 6, double mutant microspores do not resorb the vacuole (Figure 6). A cell impaired in sphingolipid biosynthesis might be expected to have defects in vacuole biogenesis given that sphingolipids are enriched in the tonoplast in plant cells (Verhoek *et al.*, 1983; Yoshida and Uemura, 1986), and altered vacuole morphology has been observed in yeast mutants that are defective in sphingolipid synthesis (Færgeman *et al.*, 2004). However, more striking phenotypes in the double mutant pollen were the reduced content of the endomembrane system components (ER and Golgi stacks), and the associated absence of the pollen wall intine layer. Loss of these primary endomembrane components is probably a major contributor to the gametophytic lethality observed in *LCB2*-null mutants. For example, deposition of the polysaccharides that comprise the intine layer requires a functional ER and Golgi system (Hess, 1993; Nakamura, 1979). Plant membrane fractions enriched in Golgi have recently been shown to contain sphingolipids (Laloi *et al.*, 2007), and alterations in sphingolipid composition have been linked with defects in membrane trafficking in Arabidopsis (Zheng *et al.*, 2005). Although there is a clear link between intine formation and a functional endomembrane system, less obvious is the relationship of the endomembrane system to other mutant phenotypic characteristics,

such as formation of vesicles in the nuclear envelope and the alteration of plastid structure, and lack of DAPI staining in the nucleus.

The gametophytic lethality of the *AtLCB2* double knockout is somewhat surprising in light of the recently reported embryo-lethal phenotype associated with a T-DNA insertion in the Arabidopsis *LCB1* gene (Chen *et al.*, 2006). Because SPT is a heteromeric enzyme with LCB1 and LCB2 subunits, null mutations in either the LCB1 or LCB2 subunits would be expected to give the same phenotype. However, this does not appear to be the case for Arabidopsis *LCB1* and *LCB2* knockouts. One possible explanation for this anomaly is that the *AtLCB1* mutant analyzed by Chen *et al.* (2006) was not a null allele. The T-DNA insertion described in this previous report is located in an intron of the *AtLCB1* gene, and it is therefore possible that a low level of LCB1 transcript accumulates in the mutant, allowing sufficient SPT activity for gametophyte development but not embryo development. An alternative explanation for the different phenotypes between the *LCB1* and *LCB2* knockouts is that the LCB1 polypeptide is sufficiently stable to allow maternally inherited LCB1 protein to persist through microspore development before LCB1 turnover depletes the level of LCB1 in the embryo. Consistent with this, studies with yeast and mammalian cells have shown that LCB2 is more subject to post-transcriptional turnover than LCB1 is (Gable *et al.*, 2000; Yasuda *et al.*, 2003), which may serve as a regulatory mechanism of SPT activity.

Inducible silencing of LCB2 demonstrates the essential nature of sphingolipids throughout sporophytic growth of Arabidopsis

As part of our studies, we developed a methoxyfenozide-inducible system for RNAi-mediated silencing of *LCB2*. The inducible RNAi construct targeted suppression of *AtLCB2b* and was introduced into an *Atlcb2a* mutant background. With this system, we showed that the lethality associated with *LCB2* silencing in seedlings could be partially rescued by inclusion of exogenous long-chain bases in the medium. This provides direct evidence that the loss of viability associated with the reduction of *LCB2* expression is due to the accompanying loss of long-chain base biosynthesis. The use of a long-chain base with an odd carbon number enabled us to demonstrate that the exogenous long-chain base is incorporated and further metabolized in the seedling. The exogenous d17:0 was shown to be further hydroxylated to form t17:0 and was also desaturated to form *cis* and *trans* isomers of d17:1 and t17:1. To our knowledge, long-chain bases with an odd number of carbon atoms have not previously been used to study sphingolipid metabolism in plants. It is likely that such molecules can be used as easily traceable probes for understanding the sequence of long-chain base modifica-

tion reactions in plants, as well as for defining the form of the substrate for these reactions (e.g. free long-chain base, ceramide). In combination with inducible silencing of *LCB2*, long-chain bases with an odd number of carbon atoms may have utility, for example, in determining the rate of sphingolipid turnover in plants cells.

Using the inducible system for silencing *LCB2* expression, it was also demonstrated that active sphingolipid synthesis is required throughout the growth of Arabidopsis, including the latter stages of growth during seed set. Silencing of *LCB2* at various stages of growth was accompanied by extensive chlorosis, initially in older leaves, that was usually evident within five days after application of the methoxyfenozide inducer. This phenotype was followed by the development of extensive necrosis and eventual senescence. Measurements of the level of long-chain bases in hydroponically grown Arabidopsis plants revealed that induction of *LCB2* silencing resulted in significant decreases in total sphingolipid content relative to induced control plants. This suggests that turnover of sphingolipids occurs in Arabidopsis, and the loss of viability accompanying *LCB2* silencing may be due, in part, to the reduced ability to replenish sphingolipids following their turnover. Based on this and prior reports of sphingolipid function, it is also likely that down-regulation of sphingolipid synthesis has an impact on endomembrane trafficking and possible regulatory functions of sphingolipids and sphingolipid metabolites (e.g. long-chain base phosphates and ceramides) in basic cellular processes (Coursol *et al.*, 2003, 2005; Liang *et al.*, 2003; Ng *et al.*, 2001; Zheng *et al.*, 2005).

Overall, our studies have provided information on the biochemical and genetic make-up of Arabidopsis SPT, and have highlighted the importance of sphingolipid biosynthesis for gametophytic and sporophytic viability. It is anticipated that the mutants and the inducible SPT silencing system will be useful for defining the cellular processes that lead to cell death under conditions of sphingolipid deficiency, and will also be useful for studies of sphingolipid metabolism in plants.

Experimental procedures

Plant material and growth conditions

For sterile growth, Arabidopsis (Col-0) seeds were surface-sterilized and sowed on half-strength MS agar plates (Sigma-Aldrich, <http://www.sigmaaldrich.com/>) containing 1% sucrose. After 2 days of stratification at 4°C, the plates were maintained under 16 h light/8 h dark conditions (120 $\mu\text{mol m}^{-2} \text{sec}^{-1}$, 23°C). Soil-grown plants were maintained at 22°C and 50% humidity under a 16 h light (100 $\mu\text{mol m}^{-2} \text{sec}^{-1}$)/8 h dark cycle. Chemical induction of RNAi transgenes was performed by foliar application of a 1/10 000 dilution of methoxyfenozide (Intrepid 2F[®], Dow Agro-Sciences; <http://www.dowagro.com>) to soil-grown plants or to the medium after autoclaving for plants maintained on MS agar plates. Inducible RNAi studies were also performed using plants

grown hydroponically as described previously (Norén *et al.*, 2004) with the addition of methoxyfenozide (1/10 000 dilution) to the medium. For complementation experiments, D-erythro-C17-sphinganine (Avanti Polar Lipids; <http://www.avantilipids.com>) was dissolved in methanol to a concentration of 5 mM and added to medium containing 0.2% Tergitol NP-40 (Sigma) to a final concentration of 200 μ M.

Genotyping of T-DNA insertion lines

SALK and SAIL T-DNA lines were obtained from the Arabidopsis Biological Research Center. For genotyping F₂ and F₃ progeny, plant tissue was collected on 96-well format CloneSaver cards (Whatman BioScience; <http://www.whatman.com>) and processed according to the manufacturer's instructions. Two separate PCR reactions were performed to genotype each allele. For SALK_061472 genotyping, the LB primer LB1a 5'-TGGTTCACGTAGTGGCCATCG-3' and the gene-specific primer 5'-GAGATTTCTCCGTCGCTTC-3' (P1) were used to test for the presence of the T-DNA, and primers P1 and 5'-AGCAGGCTTCCCAACACC-3' (P2) were used to test for homozygosity. For GABI 216-D07 genotyping, the LB primer 5'-CCCATTGGAGCTGAATGTAGACAC-3' and the gene-specific primer 5'-ACCGGAAGTTGTGGCCATATG-3' (P3) were used to test for the presence of the T-DNA, and primers P3 and 5'-TAGGCATGACTGGGGAATCAT-3' (P5) were used to test for homozygosity. For SAIL 706-A05 genotyping, the LB primer 5'-GCTTCCTATTATATCTTCCCAATTACC-3' and the gene-specific primer P5 were used to test for the presence of the T-DNA, and primers 5'-GCTCATCTTTACGCAACATCCATAC-3' (P4) and P5 were used to test for homozygosity. For SALK_110242 genotyping, LB1a and the gene-specific primer 5'-TCTGCCGAGATTGTTCAATA-3' were used to test for the presence of the T-DNA, and the primers 5'-ATCGGCGATAAAGGTTATCCTTG-3' (P6) and 5'-CCAAACATC-TCTTGAAAGAACTG-3' (P7) were used to test for homozygosity.

Vector construction

A vector for inducible RNAi silencing of *AtLCB2b* was generated using genetic elements from the previously described inducible ecdysone receptor-based system (Padidam *et al.*, 2003). The VGE element, containing the VP16 activation domain (V), GAL4 binding domain (G) and an ecdysone receptor domain (E), all under the control of the cassava mosaic virus promoter, was linked via a short spacer to a cassette containing five copies of the GAL4 response element with a minimal 35S promoter (5XG-M35S). These inducible regulatory elements were assembled in pBluescript SK+ (Stratagene, <http://www.stratagene.com/>). An *AtLCB2b*-specific RNAi inverted repeat was then introduced downstream of the 5XG-M35S cassette. The inverted repeat was prepared by PCR amplification of 286 bp encompassing primarily the 3' UTR of *AtLCB2b*, using the sense and antisense oligonucleotides 5'-CAGGTTATAAGCAAA-GCAGGTGAC-3' and 5'-GGCAACAATATATAGAGGGACACTATAC-3'. The resulting cassette containing VGE, 5XG-M35S and the *AtLCB2b* inverted repeat was introduced as an *Ascl* fragment into the pEC291 binary vector, which contains a hygromycin phosphotransferase gene for transgenic plant selection.

For yeast complementation studies, the *AtLCB2b* cDNA was cloned as an *EcoRI*/*PacI* fragment downstream of the *GAL10* promoter in the pESC-URA vector (Stratagene), alone or in combination with the *AtLCB1* cDNA under the control of the *GAL1* promoter in this vector. The *AtLCB2b* cDNA was amplified by PCR to generate the flanking restriction enzyme sites using the forward and reverse primers 5'-TTTGAATTCGAGCTGAAACAATGATTACGA-

TCC-3' and 5'-ATATTAATTAAGTGTTCCTTACGGGTTTAATCC-3'. Yeast expression plasmids containing the *AtLCB2a* and *AtLCB1* cDNAs separately or in combination were the same as previously described (Chen *et al.*, 2006).

The *AtLCB2a* and *AtLCB2b* promoter:GUS reporter constructs were generated by amplification of approximately 1.0 kb sequences upstream of their start codons using the oligonucleotides 5'-GCAAGCTTCTCAGCCAGTTGATAGATCATGC-3' (sense, *AtLCB2a*), 5'-ACTCTAGATTTCTCCAAGAACGGCTTCGTC-3' (antisense, *AtLCB2a*), 5'-GCAAGCTTGCTTTTGGAGAAGAAAAACGGTTCTATAT-3' (sense, *AtLCB2b*) and 5'-ACTCTAGATGTTTCAGCTCCGTGTTTCGTC-3' (antisense, *AtLCB2b*). The products were digested with *HindIII* and *XbaI*, and cloned into the corresponding sites of binary vector pBI121 (Clontech, <http://www.clontech.com/>) to generate a transcriptional fusion with the β -glucuronidase (GUS) coding region.

Arabidopsis transformation and selection

Binary vectors were introduced into *Agrobacterium tumefaciens* C58 by electroporation. Transgenic plants were generated by floral dip (Clough and Bent, 1998) of Arabidopsis (Col-0). Kanamycin (40 μ g ml⁻¹) and hygromycin (40 μ g ml⁻¹) in MS agar plates (see above) were used for selection of transformants for the promoter:GUS and inducible RNAi experiments, respectively.

Yeast complementation and SPT assay

Yeast complementation experiments were performed using the methods and *Saccharomyces cerevisiae* *lcb1Δ/lcb2Δ* host strain previously described by Chen *et al.* (2006). Assays of SPT activity in yeast microsomes were conducted as described by Chen *et al.* (2006).

Northern blot analysis and RT-PCR

Total RNA extraction and Northern blot analysis were performed as described by Ge *et al.* (2005). For RT-PCR analyses, total RNA was isolated using an RNeasy Plant Kit (Qiagen, <http://www.qiagen.com>) according to the manufacturer's protocol. Total RNA (1 μ g) was treated with DNase (Roche, <http://www.roche-applied-science.com>), and first-strand cDNA was subsequently synthesized using SuperScript III reverse transcriptase (Invitrogen) and oligo(dT) primer, according to the manufacturer's instructions. A 2 μ l aliquot of first-strand cDNA was used as the template for amplification with primers for *AtLCB2a*, *AtLCB2b* or the β -tubulin *TUB1* gene (At1g75780) in a 20 μ l reaction. PCR amplification (33 cycles) was performed using *Taq* DNA polymerase (New England Biolabs; <http://www.neb.com>). The primers used for amplification of *AtLCB2a* were 5'-GAGATTTCTCCGTCGCTTC-3' and 5'-AGCAGGCTTTCCCAACACC-3'. The primers used for amplification of *AtLCB2b* were 5'-ATCGGCGATAAAGGTTATCCTTG-3' and 5'-CCAAACATCTCTTGAAAGAACTG-3'. The Arabidopsis β -tubulin (*TUB1*)-specific primers were as described previously (Tsegaye *et al.*, 2007).

Staining and microscopy

The histochemical assay for GUS activity was performed according to the protocol described by Gallagher (1992). Dissected seeds and GUS-stained tissues were digitally imaged using a dissecting

microscope (Nikon SMZ 1500; <http://www.nikoninstruments.com>). Embryos were cleared with Hoyer's solution and digitally imaged using a Nikon Eclipse E800 microscope equipped with differential interference contrast (DIC) optics (Chen *et al.*, 2006). Pollen viability was assessed using Alexander's stain (Alexander, 1969) as previously described (Ge *et al.*, 2005). Pollen was stained using 4',6-diamidino-2-phenylindole (DAPI, Sigma-Aldrich) according to the method described by Park *et al.* (1998), and visualized with white light and fluorescence using a Nikon Eclipse E800 microscope with 360/40 nm bandpass excitation and 465/30 nm bandpass emission detection. For ultrastructure analysis, buds containing anthers at various developmental stages were ultra-rapidly frozen by high-pressure freezing, freeze-substituted in 2% osmium tetroxide in acetone, and embedded in Epon/Araldite as described previously (Hammes *et al.*, 2005). Thin sections stained with uranyl and lead salts were imaged digitally using a Leo 912 energy filter transmission electron microscope (Carl Zeiss; <http://www.smt.zeiss.com/leo>).

Analysis of sphingolipid long-chain bases

Lyophilized leaves (approximately 10 mg) were used for measurement of total sphingolipid long-chain base content and composition. Leaves were subjected to strong alkaline hydrolysis, and the released long-chain bases were analyzed as fluorescent derivatives by reverse-phase HPLC relative to a d16:1 internal standard as previously described (Chen *et al.*, 2006; Markham *et al.*, 2006). Identities of long-chain bases, including derivatives of d17:0, were determined by LC-MS (Chen *et al.*, 2006; Markham *et al.*, 2006).

Acknowledgements

We thank Dr Jan Jaworski, Dr Jonathan Markham and Dr Daniel Lynch (Williams College) for helpful discussions, and Ms Jia Li for technical assistance. We acknowledge the Arabidopsis Biological Research Center for providing the SALK and SAIL T-DNA mutants, Dr Roger Beachy for providing genetic elements used for the inducible expression system, and Dr Christopher Taylor for providing the backbone vector of the RNAi cassette. This work was supported by National Science Foundation Arabidopsis 2010 grant numbers MCB-0313466 to T.M.D. and MCB-0312559 to E.B.C.

Supplementary Material

The following supplementary material is available for this article online:

Table S1. Segregation analysis of F₂ progeny from plants carrying *AtLCB2* mutant alleles.

Table S2. Segregation analysis of progeny from reciprocal crosses of plants carrying mutant *AtLCB2* alleles.

Figure S1. Microarray-derived expression profiles of *AtLCB2a* and *AtLCB2b*.

Figure S2. Defects in female gametophyte development.

Figure S3. Inducible RNAi silencing of *AtLCB2b*.

Figure S4. Inducible *AtLCB2* silencing results in lethality in mature plants.

This material is available as part of the online article from <http://www.blackwell-synergy.com>.

Please note: Blackwell publishing are not responsible for the content or functionality of any supplementary materials supplied by the authors. Any queries (other than missing material) should be directed to the corresponding author for the article.

References

- Adachi-Yamada, T., Gotoh, T., Sugimura, I., Tateno, M., Nishida, Y., Onuki, T. and Date, H. (1999) *De novo* synthesis of sphingolipids is required for cell survival by down-regulating c-Jun N-terminal kinase in *Drosophila* imaginal discs. *Mol. Cell. Biol.* **19**, 7276–7286.
- Alexander, M.P. (1969) Differential staining of aborted and nonaborted pollen. *Stain Technol.* **44**, 117–122.
- Bejaoui, K., Uchida, Y., Yasuda, S., Ho, M., Nishijima, M., Brown, R.H. Jr, Holleran, W.M. and Hanada, K. (2002) Hereditary sensory neuropathy type 1 mutations confer dominant negative effects on serine palmitoyltransferase, critical for sphingolipid synthesis. *J. Clin. Invest.* **110**, 1301–1308.
- Borner, G.H., Sherrier, D.J., Weimar, T., Michaelson, L.V., Hawkins, N.D., Macaskill, A., Napier, J.A., Beale, M.H., Lilley, K.S. and Dupree, P. (2005) Analysis of detergent-resistant membranes in *Arabidopsis*. Evidence for plasma membrane lipid rafts. *Plant Physiol.* **137**, 104–116.
- Bowman, J.L., Smyth, D.R. and Meyerowitz, E.M. (1989) Genes directing flower development in *Arabidopsis*. *Plant Cell* **1**, 37–52.
- Buede, R., Rinker-Schaffer, C., Pinto, W.J., Lester, R.L. and Dickson, R.C. (1991) Cloning and characterization of LCB1, a *Saccharomyces* gene required for biosynthesis of the long-chain base component of sphingolipids. *J. Bacteriol.* **173**, 4325–4332.
- Chen, M., Han, G., Dietrich, C.R., Dunn, T.M. and Cahoon, E.B. (2006) The essential nature of sphingolipids in plants as revealed by the identification and functional characterization of the *Arabidopsis* LCB1 subunit of serine palmitoyltransferase. *Plant Cell*, **18**, 3576–3593.
- Clough, S.J. and Bent, A.F. (1998) Floral dip, a simplified method for *Agrobacterium*-mediated transformation of *Arabidopsis thaliana*. *Plant J.* **16**, 735–743.
- Coursol, S., Fan, L.M., Le Stunff, H., Spiegel, S., Gilroy, S. and Assmann, S.M. (2003) Sphingolipid signaling in *Arabidopsis* guard cells involves heterotrimeric G proteins. *Nature*, **423**, 651–654.
- Coursol, S., Le Stunff, H., Lynch, D.V., Gilroy, S., Assmann, S.M. and Spiegel, S. (2005) *Arabidopsis* sphingosine kinase and the effects of phytosphingosine-1-phosphate on stomatal aperture. *Plant Physiol.* **137**, 724–737.
- Færgeman, N.J., Feddersen, S., Christiansen, J.K., Larsen, M.K., Schneider, R., Ungermann, C., Mutenda, K., Roepstorff, P. and Knudsen, J. (2004) Acyl-CoA-binding protein, Acb1p, is required for normal vacuole function and ceramide synthesis in *Saccharomyces cerevisiae*. *Biochem. J.* **380**, 907–918.
- Gable, K., Slife, H., Bacikova, D., Monaghan, E. and Dunn, T.M. (2000) Tsc3p is an 80-amino acid protein associated with serine palmitoyltransferase and required for optimal enzyme activity. *J. Biol. Chem.* **275**, 7597–7603.
- Gable, K., Han, G., Monaghan, E., Bacikova, D., Natarajan, M., Williams, R. and Dunn, T.M. (2002) Mutations in the yeast LCB1 and LCB2 genes, including those corresponding to the hereditary sensory neuropathy type I mutations, dominantly inactivate serine palmitoyltransferase. *J. Biol. Chem.* **277**, 10194–10200.
- Gallagher, S.R. (ed.) (1992) *GUS Protocols: Using the GUS Gene as a Reporter of Gene Expression*. San Diego, CA: Academic Press.
- Ge, X., Dietrich, C.R., Matsuno, M., Li, G., Berg, H. and Xia, Y. (2005) An *Arabidopsis* aspartic protease functions as an anti-cell-death component in reproduction and embryogenesis. *EMBO Rep.* **6**, 282–288.
- Grini, P.E., Schnittger, A., Schwarz, H., Zimmermann, I., Schwab, B., Jurgens, G. and Hulskamp, M. (1999) Isolation of ethyl methanesulfonate-induced gametophytic mutants in *Arabidopsis*

- thaliana* by a segregation distortion assay using the multimarker chromosome 1. *Genetics*, **151**, 849–863.
- Hammes, U.Z., Schachtman, D.P., Berg, R.H., Nielsen, E., Koch, W., McIntyre, L.M. and Taylor, C.G. (2005) Nematode-induced changes of transporter gene expression in *Arabidopsis* roots. *Mol. Plant Microbe Interact.* **18**, 1247–1257.
- Han, G., Gable, K., Yan, L., Natarajan, M., Krishnamurthy, J., Gupta, S.D., Borovitskaya, A., Harmon, J.M. and Dunn, T.M. (2004) The topology of the Lcb1p subunit of yeast serine palmitoyltransferase. *J. Biol. Chem.* **279**, 53707–53716.
- Hanada, K. (2003) Serine palmitotransferase, a key enzyme of sphingolipids metabolism. *Biochim. Biophys. Acta*, **1632**, 16–30.
- Hanada, K., Nishijima, M., Kiso, M., Hasegawa, A., Fujita, S., Ogawa, T. and Akamatsu, Y. (1992) Sphingolipids are essential for the growth of Chinese hamster ovary cells. Restoration of the growth of a mutant defective in sphingoid base biosynthesis by exogenous sphingolipids. *J. Biol. Chem.* **267**, 23527–23533.
- Hess, M.W. (1993) Cell-wall development in freeze-fixed pollen: intine formation of *Ledebouria socialis* (Hyacinthaceae). *Planta*, **189**, 139–149.
- Ikushiro, H., Hayashi, H. and Kagamiyama, H. (2001) A water-soluble homodimeric serine palmitoyltransferase from *Sphingomonas paucimobilis* EY2395T strain. Purification, characterization, cloning, and overproduction. *J. Biol. Chem.*, **276**, 18249–18256.
- Johnson, M.A., von Besser, K., Zhou, Q., Smith, E., Aux, G., Patton, D., Levin, J.Z. and Preuss, D. (2004) *Arabidopsis hapless* mutations define essential gametophytic functions. *Genetics*, **168**, 971–982.
- Koo, J.C., Asurmendi, S., Bick, J., Woodford-Thomas, T. and Beachy, R.N. (2004) Ecdysone agonist-inducible expression of a coat protein gene from tobacco mosaic virus confers viral resistance in transgenic *Arabidopsis*. *Plant J.* **37**, 439–448.
- Laloi, M., Perret, A.M., Chatre, L. et al. (2007) Insights into the role of specific lipids in the formation and delivery of lipid microdomains to the plasma membrane of plant cells. *Plant Physiol.*, **143**, 461–472.
- Liang, H., Yao, N., Song, J.T., Luo, S., Lu, H. and Greenberg, J.T. (2003) Ceramide phosphorylation modulates programmed cell death in plants. *Genes Dev.* **17**, 2636–2641.
- Lynch, D.V. and Dunn, T.M. (2004) An introduction to plant sphingolipids and a review of recent advances in understanding their metabolism and function. *New Phytol.* **161**, 677–702.
- Markham, J.E., Li, J., Cahoon, E.B. and Jaworski, J.G. (2006) Plant sphingolipids: separation and identification of major sphingolipid classes from leaves. *J. Biol. Chem.* **281**, 22684–22694.
- Mongrand, S., Morel, J., Laroche, J., Claverol, S., Carde, J.P., Hartmann, M.A., Bonneau, M., Simon-Plas, F., Lessire, R. and Bessoule, J.J. (2004) Lipid rafts in higher plant cells: purification and characterization of Triton X-100-insoluble microdomains from tobacco plasma membrane. *J. Biol. Chem.* **279**, 36277–36286.
- Nagiec, M.M., Baltisberger, J.A., Wells, G.B., Lester, R.L. and Dickson, R.C. (1994) The LCB2 gene of *Saccharomyces* and the related LCB1 gene encode subunits of serine palmitoyltransferase, the initial enzyme in sphingolipid synthesis. *Proc. Natl Acad. Sci. USA*, **91**, 7899–7902.
- Nakamura, S. (1979) Development of the pollen grain wall in *Lolium longiflorum*. *J. Electron Microsc.* **28**, 275–284.
- Ng, C.K., Carr, K., McAinsh, M.R., Powell, B. and Hetherington, A.M. (2001) Drought-induced guard cell signal transduction involves sphingosine-1-phosphate. *Nature*, **410**, 596–599.
- Norén, H., Svensson, P. and Andersson, B. (2004) A convenient and versatile hydroponic cultivation system for *Arabidopsis thaliana*. *Physiol. Plant.* **121**, 343–348.
- Owen, H.A. and Makaroff, C.A. (1995) Ultrastructure of microsporangogenesis and microgametogenesis in *Arabidopsis thaliana* (L.) Heynh. ecotype Wassilewskija (Brassicaceae). *Protoplasma*, **185**, 7–21.
- Padidam, M., Gore, M., Lu, D.L. and Smirnova, O. (2003) Chemical-inducible, ecdysone receptor-based gene expression system for plants. *Transgenic Res.* **12**, 101–119.
- Park, S.K., Howden, R. and Twell, D. (1998) The *Arabidopsis thaliana* gametophytic mutation *geminipollen1* disrupts microspore polarity, division asymmetry and pollen cell fate. *Development*, **125**, 3789–3799.
- Spassieva, S.D., Markham, J.E. and Hille, J. (2002) The plant disease resistance gene *Asc-1* prevents disruption of sphingolipid metabolism during AAL-toxin-induced programmed cell death. *Plant J.* **32**, 561–572.
- Sperling, P., Franke, S., Luthje, S. and Heinz, E. (2005) Are glucocerebrosides the predominant sphingolipids in plant plasma membranes? *Plant Physiol. Biochem.* **43**, 1031–1038.
- Tamura, K., Musuhashi, M., Hara-Nishimura, I. and Imai, H. (2001) Characterization of an *Arabidopsis* cDNA encoding a subunit of serine palmitoyltransferase, the initial enzyme in sphingolipid biosynthesis. *Plant Cell Physiol.* **42**, 1271–1281.
- Townley, H.E., McDonald, K., Jenkins, G.I., Knight, M.R. and Leaver, C.J. (2005) Ceramides induce programmed cell death in *Arabidopsis* cells in a calcium dependent manner. *Biol. Chem.* **386**, 161–166.
- Tsegaye, Y., Richardson, C.G., Bravo, J.E., Mulcahy, B.J., Lynch, D.V., Markham, J.E., Jaworski, J.G., Chen, M., Cahoon, E.B. and Dunn, T.M. (2007) *Arabidopsis* mutants lacking long chain base phosphate lyase are fumonisin-sensitive and accumulate trihydroxy-18:1 long chain base phosphate. *J. Biol. Chem.* **282**, 28195–28206.
- Verhoek, B., Haas, R., Wrage, K., Linscheid, M. and Heinz, E. (1983) Lipids and enzymatic activities in vacuolar membranes isolated via protoplasts from oat primary leaves. *Z. Naturforsch.* **38c**, 770–777.
- Voinnet, O., Vain, P., Angell, S. and Baulcombe, D.C. (1998) Systemic spread of sequence-specific transgene RNA degradation in plants is initiated by localized introduction of ectopic promoterless DNA. *Cell*, **95**, 177–187.
- Wang, H., Li, J., Bostock, R.M. and Gilchrist, D.G. (1996) Apoptosis: a functional paradigm for programmed plant cell death induced by a host-selective phytotoxin and invoked during development. *Plant Cell*, **8**, 375–391.
- Yamamoto, Y., Nishimura, M., Hara-Nishimura, I. and Noguchi, T. (2003) Behavior of vacuoles during microspore and pollen development in *Arabidopsis thaliana*. *Plant Cell Physiol.* **44**, 1192–1201.
- Yasuda, S., Nishijima, M. and Hanada, K. (2003) Localization, topology, and function of the LCB1 subunit of serine palmitoyltransferase in mammalian cells. *J. Biol. Chem.* **278**, 4176–4183.
- Yoshida, S. and Uemura, M. (1986) Lipid composition of plasma membranes and tonoplasts isolated from etiolated mung bean (*Vigna radiata* L.). *Plant Physiol.* **82**, 807–812.
- Zhang, K., Showalter, M., Revollo, J., Hsu, F.F., Turk, J. and Beverley, S.M. (2003) Sphingolipids are essential for differentiation but not growth in *Leishmania*. *EMBO J.* **22**, 6016–6026.
- Zheng, H., Rowland, O. and Kunst, L. (2005) Disruptions of the *Arabidopsis* enoyl-CoA reductase gene reveal an essential role for very-long-chain fatty acid synthesis in cell expansion during plant morphogenesis. *Plant Cell*, **17**, 1467–1481.
- Zimmermann, P., Hirsch-Hoffmann, M., Hennig, L. and Gruissem, W. (2004) GENEVESTIGATOR. *Arabidopsis* microarray database and analysis toolbox. *Plant Physiol.* **136**, 2621–2632.